

Received 25 September 2025, accepted 14 November 2025, date of publication 19 November 2025,
date of current version 25 November 2025.

Digital Object Identifier 10.1109/ACCESS.2025.3634717

RESEARCH ARTICLE

Quantum-Accelerated Feature Selection for Edge-Enabled Perception in Connected and Autonomous Vehicles

VIKAS HASSIJA¹, AVISHIKTA BHATTACHARJEE¹, ARADHYA CHAKRABARTI¹,
QAISER RAZI², (Graduate Student Member, IEEE), M. ADHITYA¹,
AND G. S. S. CHALAPATHI², (Senior Member, IEEE)

¹School of Computer Engineering, Kalinga Institute of Industrial Technology (KIIT), Bhubaneswar 751024, India

²Department of Electrical and Electronics Engineering, Birla Institute of Technology and Science, Pilani, Vidyavihar, Pilani, Rajasthan 333031, India

Corresponding author: Vikas Hassija (vikas.hassijafcs@kiit.ac.in)

ABSTRACT The growing complexity and volume of traffic and sensory data in Connected and Autonomous Vehicles (CAVs) make it crucial to develop more effective methods for selecting and extracting features from high-dimensional images and videos. This paper proposes a novel quantum-accelerated feature selection framework utilising the Variational Quantum Eigensolver (VQE) to enhance perception tasks in CAV environments. By decomposing high-dimensional traffic images into compact patches encoded as quantum Hamiltonians, the proposed design aims to support Intelligent Transportation Systems (ITS) tasks such as object detection, vehicle classification, and traffic monitoring in CAVs. The quantum hybrid method serves as a pipeline for extracting selective features that have been optimised using gradient-aware parameter pruning and conditional principal component analysis (PCA). The implementation of this quantum hybrid approach facilitates addressing computational challenges at the edge in embedded vehicular systems, reducing data dimensionality while preserving key discriminative spatial patterns necessary for object detection and traffic monitoring. Although the quantum method currently underperforms in certain clustering and separability metrics, it demonstrates potential as a viable alternative for advanced perception in CAVs. This work lays a foundation for integrating quantum computing into edge-based autonomous vehicle perception, highlighting both opportunities and challenges with near-term quantum hardware.

INDEX TERMS Variational quantum eigensolver, pruning, feature selection, machine learning, quantum computing, connected autonomous vehicles (CAVs).

I. INTRODUCTION

The rapid growth of Intelligent Transportation Systems (ITS) and autonomous vehicles has led to an explosion in the volume and complexity of traffic data. ITS uses a wide array of communication, control, vehicle detection, and electronic technologies to address and manage the challenges caused by growing traffic volumes [1]. Connected autonomous vehicles (CAVs) generate massive amounts of data that require reliable and low-latency transmission to ensure safe and efficient driving. However, limited wireless

communication resources and high vehicle mobility pose significant challenges in meeting these rigid requirements, often leading to network congestion and packet loss [2]. The above challenges can be addressed using state-of-the-art technology, focusing on integrating deep learning models such as hybrid CNN-transformer architectures to improve feature representation and sensitivity to small objects. These methods often employ specialised modules like upsampling-based small-object detection layers and advanced loss functions (e.g., SIOU) to boost detection accuracy and computational efficiency. Moreover, techniques such as radio tomographic imaging have shown promise for multi-object localisation in noncooperative environments, providing robust performance

The associate editor coordinating the review of this manuscript and approving it for publication was Jiankang Zhang¹.

even in the presence of noise and without the need for object-specific tags [3]. However, such enhancements can increase the computational complexity and parameter count, potentially affecting real-time performance, especially on edge devices with limited resources. As a result, lightweight model designs and efficient feature mapping techniques have become essential for achieving a balance between detection accuracy and real-time feasibility in embedded vehicular applications [4], [5].

Quantum computing provides unconventional methods for processing large-scale data by exploiting quantum phenomena such as entanglement, superposition, and nonlocal information encoding, enabling efficiencies unattainable by classical systems. The integration of advanced resource allocation strategies, including those based on quantum reinforcement learning and blockchain technologies, offers a promising direction to enhance both the security and efficiency of vehicular edge computing systems [6]. Encoding traffic images and videos using quantum states allows higher compression rates, faster pattern extraction, and more efficient analysis compared to classical frameworks [7]. Variational Quantum Eigensolver (VQE)-based approaches generally have a time complexity of the order $\sim \mathcal{O}(n^3)$, as compared to classical eigenvalue solvers, which have a time complexity of the order $\sim \mathcal{O}(2^n)$.

Quantum feature extraction methods, particularly the VQE [8], offer a hybrid approach for estimating ground states of Hamiltonians, capturing essential structural information for downstream tasks. VQE optimises a quantum circuit to minimise the expected value of an energy function. The expectation is always greater than or equal to the true ground state energy, i.e:

$$\langle \psi | H | \psi \rangle \geq E_0 \quad (1)$$

Beyond quantum computational advantages, integrating quantum communication protocols with edge-enabled CAV systems presents significant opportunities for secure data transmission. Quantum-Enhanced Edge Computing frameworks combine quantum communication principles with edge processing to address critical vehicular network challenges, including secure vehicle-to-vehicle (V2V) and vehicle-to-infrastructure (V2I) communications. Furthermore, quantum communication networks enable distributed quantum sensing and collaborative feature extraction across vehicle fleets, where quantum entanglement facilitates coordinated perception tasks. The proposed feature selection framework naturally complements these quantum communication capabilities by reducing the dimensional burden of data transmitted between edge nodes, creating synergies between quantum computation and quantum communication in the CAV ecosystem.

The major contributions of the work are discussed as follows:

- A variational quantum circuit is proposed to estimate the ground state of a Hamiltonian using VQE for data representation.

- Ground state solutions are used to extract compressed, information-rich features from high-dimensional traffic image and video data.
- A hybrid dimensionality reduction scheme combining classical prefiltering, parameter pruning, and conditionally applied PCA is used to optimise feature spaces.
- Experimental results demonstrate that quantum approaches achieve feasible performance for image and video analysis, though further optimisation is required to rival classical methods. This may be utilised for traffic monitoring to detect objects in large-scale multidimensional traffic scenes.

II. RELATED WORK

This section reviews the current state of classical feature selection methods and their limitations in CAV environments, and examines the feasibility of emerging quantum computing solutions for addressing these challenges.

A. CLASSICAL FEATURE SELECTION METHODS

In the domain of ITS, robust vehicle detection under diverse and challenging conditions remains a primary focus, with various advanced computational methods being explored. Early example-based approaches, such as the work by Zhou et al. [9], utilized classical machine learning pipelines combining Principal Component Analysis (PCA) for feature extraction from image histograms and Support Vector Machines (SVM) for classifying image blocks as parts of a vehicle, effectively handling variations in illumination and shadows. More recent techniques have integrated deep learning; for instance, Yao et al. [10] proposed a coupled framework that combines a prior objectness measure to efficiently generate high-quality vehicle proposals with a Convolutional Neural Network (CNN) to simultaneously detect and classify multiple vehicle types, significantly reducing search time compared to sliding-window methods. For specialised surveillance applications, Zhang et al. [11] developed a vision-based vehicle detection method for VideoSAR that employs low-rank plus sparse three-term decomposition (TTD) to isolate moving vehicles from the background and sensor noise, demonstrating efficacy in single-channel configurations.

B. LIMITATIONS OF CLASSICAL APPROACHES IN CAV CONTEXT

Classical feature selection methods face unprecedented challenges when applied to CAV high-dimensional sensor data, where the curse of dimensionality significantly affects traditional approaches as CAV systems generate vast amounts of heterogeneous data from LiDAR, cameras, radar, and GPS sensors that create sparse feature spaces where distance-based algorithms become ineffective. Traditional wrapper methods, which evaluate different feature combinations through exhaustive search, become computationally intractable with CAV's high-dimensional datasets, while

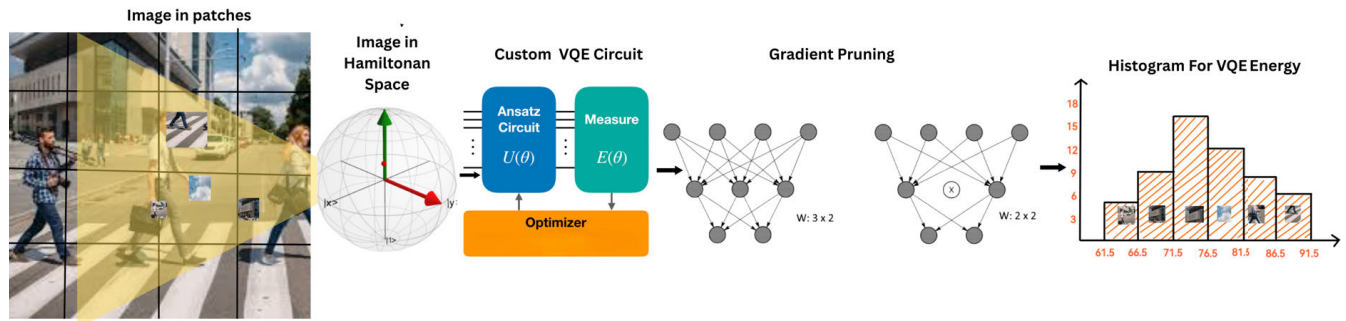


FIGURE 1. System model for proposed framework.

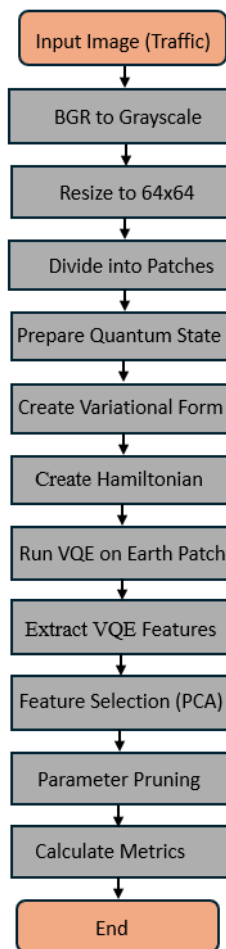


FIGURE 2. Workflow of the proposed method.

filter methods, though faster, fail to model complex feature dependencies and interactions critical for autonomous driving perception tasks. The exponential growth in computational complexity with increasing feature dimensions makes classical approaches unsuitable for real-time vehicular applications that demand millisecond-level decision making, which conflicts with the computational overhead of traditional methods. High-dimensional CAV sensor data with

limited training samples leads to overfitting issues where classical feature selection methods pick up noise and random fluctuations rather than meaningful patterns, resulting in poor generalisation across different driving environments, weather conditions, and geographical locations. Furthermore, classical approaches struggle to handle the heterogeneous nature of CAV sensor data, where features from different modalities require sophisticated fusion techniques that traditional methods cannot effectively address, leading to suboptimal feature selection outcomes. These fundamental limitations necessitate quantum-accelerated approaches that can handle the exponential complexity of CAV feature spaces while maintaining the real-time processing capabilities essential for safe autonomous driving operations [12].

C. QUANTUM COMPUTING SOLUTIONS FOR FEATURE SELECTION

Several researchers have explored the integration of quantum computing into feature selection and dimensionality reduction tasks. Mücke et al. [13] proposed a feature selection algorithm by formulating the problem as a Quadratic Unconstrained Binary Optimisation (QUBO) instance, enabling the simultaneous optimisation of feature importance and redundancy. Unlike iterative or greedy strategies, their direct formulation method produces high-quality, globally optimised feature subsets without needing multiple optimisation rounds [14]. Similarly, Turati et al. [15] formulated feature selection as a QUBO and mapped it to an Ising Hamiltonian to leverage the Quantum Approximate Optimisation Algorithm (QAOA). Their experiments showed that even with limited quantum resources, QAOA-based feature selection can perform competitively on real-world datasets, though they noted that optimising classical components such as parameter initialisation and mixer Hamiltonian design could further enhance performance.

Expanding on quantum-assisted feature selection, Wang [16] introduced the Quantum Support Vector Machine Feature Selection (QSVMF) method. QSVMF integrates quantum SVM classifiers with a multi-objective genetic algorithm to simultaneously optimise for high classification accuracy, minimal feature subset size, low redundancy,

and reduced quantum circuit complexity. Their work emphasises that optimising multiple competing objectives is crucial in practical quantum machine learning systems where resources like qubits and circuit depth are limited. In a complementary direction, Gong [17] proposed a variational quantum isometric mapping approach aimed at nonlinear dimensionality reduction. Their method combines quantum k-nearest neighbors (k-NN) for geodesic distance computation with the Variational Quantum Eigensolver (VQE) to learn low-dimensional embeddings while preserving local structures. Furthermore, Nath et al. [18] utilised quantum annealing to perform robust feature subset selection in the context of physiological stress detection.

D. ADDRESSING CAV CHALLENGES THROUGH QUANTUM METHODS

Connected and Autonomous Vehicles (CAVs) face critical challenges that quantum computing methods can address through fundamentally different computational paradigms. Two primary quantum approaches demonstrate significant potential for overcoming CAV limitations: quantum-accelerated feature selection and quantum secure communication protocols. For example, Quantum Key Distribution (QKD) establishes unconditionally secure communication channels between CAVs and infrastructure by exploiting quantum mechanical principles. Unlike classical encryption, vulnerable to quantum computers, QKD's physics-based security automatically detects eavesdropping attempts through quantum state disturbance. Additionally, Quantum Random Number Generation strengthens cryptographic key generation, ensuring robust entropy for automotive hardware security modules [19]. Grover's quantum search algorithm provides a quadratic speedup for CAV network optimisation problems, enabling efficient routing, resource allocation, and real-time decision-making that classical methods find computationally intractable. Quantum feature selection emerges as crucial for processing high-dimensional sensor data from LiDAR, cameras, radar, and GPS systems. Quantum annealing-based algorithms solve Quadratic Unconstrained Binary Optimisation problems to identify optimal feature subsets, maximising mutual information while minimising redundancy. This dramatically improves machine learning model performance for object detection, path planning, and collision avoidance while reducing computational costs [20].

The convergence of quantum technologies with CAV systems represents a fundamental paradigm shift toward truly secure, intelligent autonomous transportation, offering unprecedented protection against emerging cyber threats while enhancing operational efficiency and safety.

III. METHODOLOGY

A. SYSTEM WORKFLOW

This paper proposes a new hybrid quantum-classical feature extraction pipeline tailored for high-dimensional image and video data, as shown in Fig. 1. Our method begins with

a variational quantum circuit (VQC) that is trained to approximate the ground state of a carefully constructed Hamiltonian representing the dataset's feature space. The low-energy ground states generated by the VQC yield compressed, information-rich representations that preserve essential class-discriminative features. To further refine the feature set, a lightweight classical prefiltering step removes redundant parameters, followed by a conditional Principal Component Analysis (PCA) stage to ensure orthogonality and further dimensionality reduction if necessary. The design intentionally balances quantum circuit complexity and feature informativeness, ensuring compatibility with near-term noisy quantum hardware. Here, Fig. 2 illustrates the steps involved in the proposed model. The proposed algorithm for feature extraction and selection uses the aforementioned classical-quantum hybrid approach. Note that all simulations are carried out using the IBM Qiskit software development kit to work with quantum computers in Python.

B. PRE-PROCESSING

Images are used as input data and are first normalised to grayscale. Instead of directly feeding the full image array for feature selection, the image is divided into smaller patches. The quantum state initialisation is then performed for each 4×4 patch as follows:

$$|\psi_{\text{patch}}\rangle = \bigotimes_{i=1}^{16} RY(\arccos(x_i))|0\rangle \quad (2)$$

where,

- x_i = Normalized pixel intensity

The fidelity measure that quantifies information loss during PCA reduction is defined as follows:

$$\mathcal{F} = |\langle \psi_{\text{patch}} | \psi_{\text{reconstructed}} \rangle|^2 \quad (3)$$

The quantum VQE method restricts the input size, thereby making the direct use of the entire image impractical due to the resulting circuit complexity. Consequently, the image is processed patch by patch, with each patch representing a feature. The array containing the patch information is flattened into a two-dimensional array. Before being processed by the quantum circuit, Principal Component Analysis (PCA) is conditionally applied to the flattened patches. Specifically, PCA is implemented if the intended number of principal components is less than the number of features in the flattened patch, which corresponds to the number of pixels in the patch. The covariance matrix used for PCA is defined as follows. For a zero-centred data matrix X , the principal components are computed using:

$$\Sigma = \frac{1}{n} X^T X \quad (4)$$

The flattened 16-pixel patches are subsequently projected into a reduced PCA space using the principal component scores. For weights w (eigenvectors) and a data vector \mathbf{x}_i ,

Algorithm 1 Feature Extraction of Traffic Obstacles Using VQE and Adaptive Pruning

Input: Grayscale image I of size 64×64

Output: Selected quantum features θ , energy histograms $P(E)$ and $P(E')$, cluster metrics s, f

- 1: Load image path and resize to $(64,64)$
- 2: Extract 4×4 patches with stride 2 (50% overlap)
- 3: Apply PCA using covariance matrix using Equation (4)
- 4: Normalizing the 4×4 patches with a scale to $[-1, 1]$
- 5: **Begin Quantum Hamiltonian Construction:**
- 6: **for** each patch **do**
- 7: Construct Pauli-Y Hamiltonian using Equation (7)
- 8: Initialize parameterized quantum circuit with RY rotations.
- 9: Extract energy values $\text{Energy}_{\text{pruned}}$ using

$$\langle E \rangle = \langle \psi(\theta) | \mathcal{H}_i | \psi(\theta) \rangle$$
- 10: **end for**
- 11: **Performing VQE Optimization and Adaptive Pruning:**
- 12: **for** epoch = 1 to 100 **do**
- 13: **for** each patch **do**
- 14: Calculate the pruning threshold as the 20th percentile of absolute gradient magnitudes across all parameters.
- 15: Identify active parameters as those whose gradient magnitudes meet or exceed this threshold.
- 16: Update only the retained parameters by subtracting the product of the learning rate and their respective gradients from the current parameter values.
- 17: Terminate the optimisation process if the absolute difference in energy values between consecutive iterations falls below a predefined tolerance threshold
- 18: **end for**
- 19: **end for**
- 20: **Feature Analysis:**
- 21: Compute energy probabilities using equation (18)
- 22: Evaluate clustering metrics (Silhouette Score (s) and Fisher Ratio (f)):

$$s = \frac{b - a}{\max(a, b)}, \quad f = \frac{\text{Var}_{\text{inter}}}{\text{Var}_{\text{intra}}}$$
- 23: Plot histograms for $P(E)$ and $P(E')$

Notation: θ = circuit parameters, Y = Pauli-Y operator, a , b = intra- and inter-cluster distances, s = Silhouette score, f = Fisher ratio.

the following method is employed:

$$t_i^{(1)} = \mathbf{x}_i \cdot \mathbf{w}^{(1)} \quad (5)$$

To make sure the characteristics are within an appropriate range for encoding into the quantum circuit, this reduced

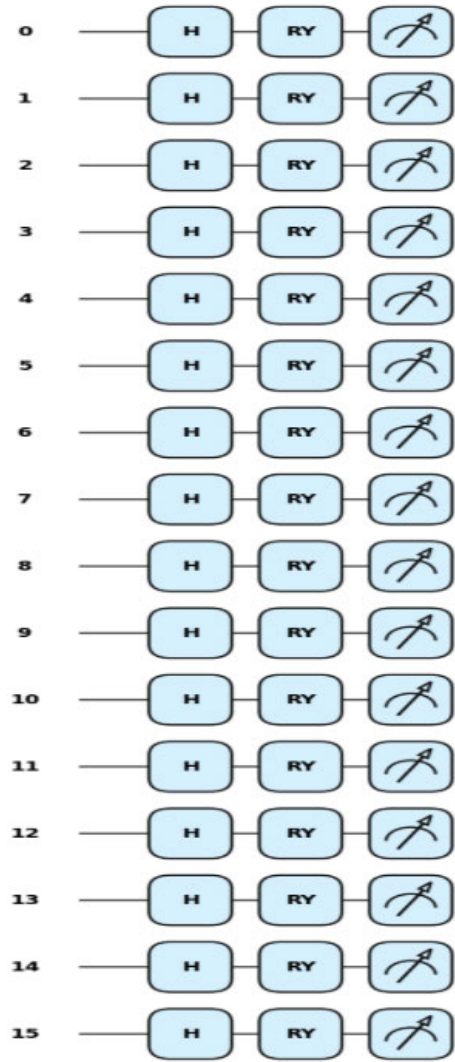


FIGURE 3. Implemented VQE circuit design.

representation is then normalised by dividing by its greatest absolute value. If the number of components is more than or equal to the original patch size, PCA is omitted, and the original flattened patch is normalised straight away. As a dimensionality reduction method, this conditional PCA application may reduce the input size of the quantum circuit and highlight the salient characteristics of each image patch.

C. HAMILTONIAN AND VARIATIONAL CIRCUIT CONSTRUCTION

The normalised patch vector is mapped to a Hamiltonian using Pauli-Z operators to encode spatial correlations. For an image patch with n pixels, the Hamiltonian is constructed as:

$$\mathcal{H} = \sum_{i=0}^{n-1} w_i Z_i + \sum_{i < j} w_{ij} Z_i \otimes Z_j + \sum_{i < j < k} w_{ijk} Z_i \otimes Z_j \otimes Z_k \quad (6)$$

where,

- $Z_i \otimes Z_j \otimes Z_k$ = Three-qubit interactions for higher-order pixel dependencies (e.g., texture patterns)
- w_i, w_{ij}, w_{ijk} = Coefficients derived from normalized PCA components and patch intensity gradients

This Hamiltonian is Hermitian by construction, as required for quantum algorithms. It encodes spatial pixel relationships from PCA-reduced features:

$$\mathcal{H} = \sum_{i=0}^{n-1} w_i Z_i + \sum_{i<j} w_{ij} Z_i \otimes Z_j \quad (7)$$

where,

- Z_i = Single-qubit Pauli-Z operator for pixel intensity variance
- $Z_i \otimes Z_j$ = Two-qubit interaction for pixel correlations
- Weights w_i, w_{ij} derived from normalized PCA components.

Unlike quantum chemistry applications [8], where Pauli operators are weighted by molecular integrals reflecting electron interactions and symmetries, here the coefficients directly represent spatial image features, and there is no need for chemistry-specific mappings or symmetries. The feature extraction utilises a variational quantum circuit (ansatz) as shown in Fig. 3, which is built from alternating layers of parameterised Ry rotation gates and CZ entangling gates, ensuring both expressivity and entanglement across the qubits representing the patch. A parameterised quantum state (ansatz) is typically denoted as follows:

$$|\psi(\theta)\rangle = U(\theta)|0\rangle \quad (8)$$

where,

- $U(\theta)$ = Unitary operator
- θ = Ansatz parameter
- $|0\rangle$ = Initial state

The parameters θ are further optimised to minimise the expectation value.

The expectation value of the predefined Hamiltonian H with respect to a quantum state $|\psi\rangle$ prepared by the circuit is described as follows:

$$\langle H \rangle_\psi = \langle \psi | H | \psi \rangle \quad (9)$$

The circuit preserves real amplitudes, restricting qubit states to the xz -plane on the Bloch sphere, which is sufficient for image data lacking complex phase dependencies. This contrasts with chemistry-focused ansatz-like Unitary Coupled Cluster (UCC), which requires R_x/R_z rotations to model complex wavefunctions. The TwoLocal ansatz employs linear entanglement with controlled-Z (CZ) gates to model spatial correlations between qubits, mirroring pixel relationships in image processing tasks. For 16 qubits, linear entanglement pairs adjacent qubits as follows:

$$CZ_{i,i+1} = |0\rangle\langle 0| \otimes I + |1\rangle\langle 1| \otimes Z \quad (10)$$

Here, $RY(\theta)$ rotations are defined as follows:

$$RY(\theta) = e^{-i\theta Y/2} \quad (11)$$

The alternating layers of RY rotations and CZ gates make the circuit both flexible and trainable. The RY rotations encode single-qubit features (pixel intensities), while the CZ gates entangle neighbouring qubits to capture spatial correlations such as edge gradients. The circuit is then optimised using a classical optimiser to minimise the expectation value of the constructed Hamiltonian. The cost function for VQE optimisation is defined as follows:

$$C(\theta) = \langle \psi(\theta) | \mathcal{H} | \psi(\theta) \rangle + \lambda \|\theta\|_1 \quad (12)$$

where,

- $\lambda \|\theta\|_1$ = L1 regularization term

The parameter-shift rule allows gradient-based optimisation directly on quantum hardware, helping find the best set of parameters that capture the key features of each image patch. The final optimised parameters act as a compact feature vector for the patch, preserving important spatial information in a way that's ready for machine learning tasks. This makes the feature selection process more efficient and brings quantum advantages to image-based applications like ITS.

Algorithm 2 Feature Extraction and Comparison of Traffic Obstacles using VQE

Input: Feature Vector from Algorithm 1

Output: Euclidian distances D_{unpruned} , D_{pruned} of two image vectors indicating similarities

- 1: Initialising Feature Vector Construction (*Per image*)
- 2: Extract energy values $\text{Energy}_{\text{pruned}}$, $\text{Energy}_{\text{unpruned}}$
- 3: Compute statistical features as:

$$\mathbf{v} = \begin{bmatrix} \mu(\text{Energy}) \\ \sigma(\text{Energy}) \\ \text{median}(\text{Energy}) \\ \min(\text{Energy}) \\ \max(\text{Energy}) \end{bmatrix}$$

- 4: Compute unpruned distance with equation (22):

$$D_{\text{unpruned}} = \|\mathbf{v}_1^{(\text{unpruned})} - \mathbf{v}_2^{(\text{unpruned})}\|_2$$

- 5: Compute pruned distance with equation (22):

$$D_{\text{pruned}} = \|\mathbf{v}_1^{(\text{pruned})} - \mathbf{v}_2^{(\text{pruned})}\|_2$$

- 6: Comparing Similarities between 2 Images by the output: D_{unpruned} , D_{pruned}

Notation:

- $\mathbf{v}_1, \mathbf{v}_2$: Feature vectors from images 1 and 2
 - $\|\cdot\|_2$: Euclidean norm
 - D_{unpruned} : Distance without parameter pruning
 - D_{pruned} : Distance with 20% parameter pruning
-

D. ENERGY PRUNING

As previously demonstrated, due to the constraints of VQE implementation, classical feature selection methods cannot be directly applied. Therefore, feature relevance is explored through the analysis of energy distributions. By processing image patches and obtaining their corresponding energy values from the VQE, histograms are generated to visualise the quantum representations of these local features. To further examine the impact of parameter choices within the quantum circuit [21], both *pruned* and *unpruned* data values are created from the same input image. A gradient magnitude-based parameter pruning technique is used, which removes less important parameters based on the size of their gradients. For a parameter vector $\theta \in \mathbb{R}^n$, the gradient can be defined as:

$$g_i = \frac{\partial \mathcal{L}}{\partial \theta_i} \quad \text{for } i = 1, 2, \dots, n \quad (13)$$

where,

- \mathcal{L} = VQE Energy loss function

These gradients are converted to absolute values to focus on their magnitudes rather than direction, where parameters with small magnitudes are considered less critical for optimisation as follows:

$$|g_i| = \left| \frac{\partial \mathcal{L}}{\partial \theta_i} \right| \quad (14)$$

The *unpruned* data represents the energy distribution obtained from a VQE circuit with the full set of parameters, while the *pruned* data comes from a circuit where less impactful parameters, identified through gradient analysis, have been removed. The *pruned* and *unpruned* data sets are distinguished using percentile thresholding. A threshold T is defined as the 20th percentile of gradient magnitudes, as follows:

$$T = \text{Percentile}(|g|, 20\%) \quad (15)$$

These parameters are pruned if their gradient magnitudes fall below T , that is:

$$\text{Pruned}_i = \begin{cases} 1 & \text{if } |g_i| \geq T \\ 0 & \text{otherwise} \end{cases} \quad (16)$$

Comparing the energy distributions of the *pruned* and *unpruned* scenarios allows us to infer the significance of different aspects of the quantum circuit in representing image features [21]. This comparison helps determine which components are more important for downstream tasks like classification, without relying on traditional classical feature selection methods. A parameter update is then applied, retaining only the *unpruned* parameters by performing element-wise multiplication with the mask, as defined below:

$$\theta_{\text{pruned}} = \theta \odot \text{Pruned} \quad (17)$$

where,

- \odot denotes element-wise multiplication.

E. PATCH-BASED ENERGY EXTRACTION

Fig.5 shows the obtained energy distributions from a sample traffic image consisting of a pedestrian in Fig.4. The differences observed in the distributions are due to the inherent characteristics of the proposed method. However, a general similarity can still be observed between the two. The histograms visualize $P(k)$ distributions from repeated VQE measurements, where:

The concentration around specific energy (E_k) values indicates latent clustering in the Hamiltonian's eigenbasis. The variance is calculated as follows:

$$\sigma_H^2 = \langle H^2 \rangle - \langle H \rangle^2 \quad (18)$$

The variance measures feature stability, with lower values, as shown in Fig.5, indicating reliable encoding. Both distributions generated from a common image at two different times show distinct clusters instead of uniform spreads, suggesting that VQE identifies natural groupings in image data. While the distributions differ, they share similar energy ranges (-1.5 to 3.0), showing stability in the algorithm. These energy plots condense high-dimensional image patches into a single value, offering much higher compression than classical feature vectors, which usually need multiple dimensions. The differences between distributions highlight how quantum circuits can explore diverse solutions, providing richer feature representations than classical methods. These energy distributions could improve transportation image processing by:

- Identifying features like traffic signs and lane markings.
- Reducing the computational load on vehicle edge devices.
- Offering noise-resistant features in bad weather.
- Enabling faster real-time processing with extreme dimensionality reduction.

F. ADDRESSING COMPUTATIONAL CONSTRAINTS

The current implementation faces significant resource constraints that limit real-world applicability. Experiments are constrained to four-by-four grayscale patches processed through basic VQE with parameter pruning, representing only proof-of-concept validation. This limitation stems from NISQ device restrictions, including limited qubit counts, short coherence times, and high gate error rates that prevent processing of larger, more realistic image data typical in automotive scenarios.

As with all quantum research in the NISQ, our classical simulation results represent an essential first step toward understanding algorithm behavior, though real quantum hardware deployment will involve additional considerations like incorporating device-specific noise profiles for enhanced robustness, leveraging the expanding qubit counts available in current systems compared to classical simulation constraints (30-40 qubits), optimising circuit depth strategies tailored to device coherence characteristics and implementing error mitigation techniques that complement hardware capabilities.

Despite these limitations, the quantum approach offers unique theoretical advantages through superposition-enabled exploration of exponentially large feature spaces simultaneously, potentially capturing non-linear relationships and entangled data patterns inaccessible to classical linear models, particularly excelling in probability-driven pattern recognition tasks where quantum parallelism provides computational advantages for high-dimensional optimisation problems.

IV. RESULTS

A. EFFECTS OF ENERGY PRUNING ON FEATURE SELECTION

The proposed methodology is carried out on two sample pedestrian images within traffic to compare and analyse the effectiveness of the workflow in Figures 6 and 9.



FIGURE 4. Pedestrian image A used as a traffic object.

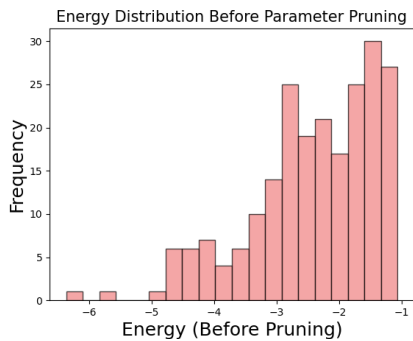


FIGURE 5. Energy distribution before pruning of image in Fig. 4.

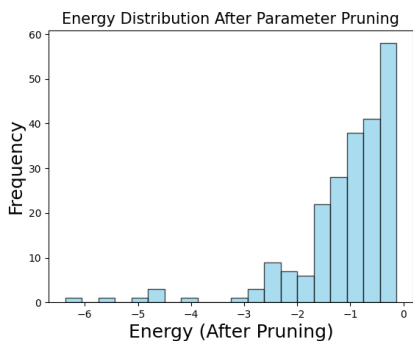


FIGURE 6. Energy distribution after pruning of the image in Fig. 4.



FIGURE 7. Pedestrian image B used as a traffic object.

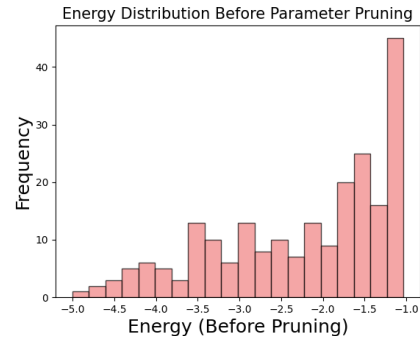


FIGURE 8. Energy distribution before pruning of image in Fig. 7.

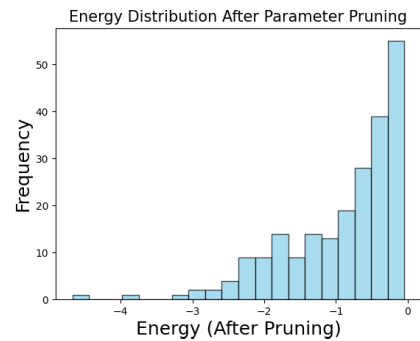


FIGURE 9. Energy distribution after pruning of image in Fig. 7.

The Euclidean distance between the two feature vectors computed before and after pruning, respectively, for the two pedestrian images, is calculated as follows:

$$d = \|\mathbf{f}_1 - \mathbf{f}_2\|_2 = \sqrt{\sum_{i=1}^n (f_{1,i} - f_{2,i})^2} \quad (19)$$

For the image in Fig. 9, the following distances in Table 1 were calculated: The decrease in distance after pruning suggests that the features became more similar. This indicates that pruning reduces the distinction between the two

TABLE 1. Euclidean distance between two feature vectors.

	Distance
Pruned	0.0841
Unpruned	0.2027

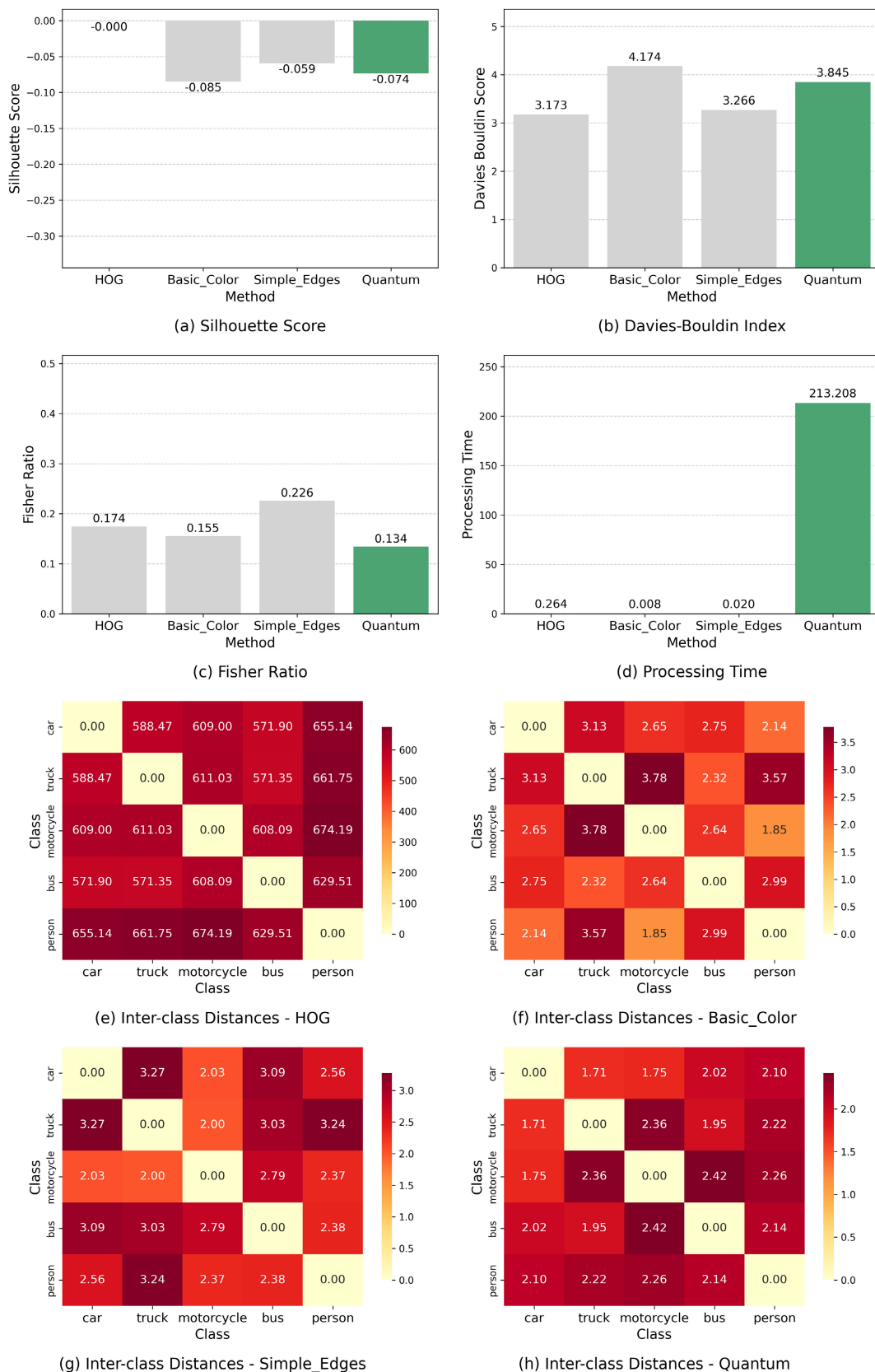


FIGURE 10. Comparison with Classical Methods (HOG, Colour-based, Edge-based): w.r.t (a) Silhouette Score, (b) Davies-Bouldin Index, (c) Fisher Ratio, (d) Processing Time (in seconds). Inter-class distances for (e) HOG method, (f) Colour-based method, (g) Edge-based method, (h) proposed Quantum-based method.

images, removing less informative features, and possibly identifying similar objects in the images of pedestrians for classification.

The absolute minimum energy for each patch's quantum representation is found by analysing the plotted expected energy. The unpruned graphs show a narrow energy distribution with an exponential rise, while pruning reduces lower-energy values, suggesting they are less significant to the image. Some features saw energy increases after pruning, which may indicate overfitting or a shift to more relevant information. The pruning process challenges traditional feature selection, as it retains higher-energy features, which are likely more informative. These energy changes offer insights into the quantum feature extraction process, showing how pruning affects feature representation, with implications for tasks like classification and object detection.

B. COMPARISON WITH CLASSICAL METHODS

Within the implementation of the workflow, a comparative analysis of image feature extraction techniques, with a particular focus on evaluating a Variational Quantum Eigensolver (VQE)-based method against several classical approaches, namely Histogram of Oriented Gradients (HOG) [22], basic colour histograms, and simple edge detection, is carried out. The comparison is structured around assessing the quality and characteristics of the feature sets generated by each method for traffic images containing objects belonging to five separate categories, i.e., *car*, *truck*, *motorcycle*, *bus* and *person*. To this end, several quantitative metrics that describe the discriminative power and efficiency of each technique are employed, especially to measure clustering abilities. These metrics include the Silhouette Score [23], the Davies-Bouldin Index [24], the Fisher Ratio [25], feature variance, feature dimensionality, and simulated quantum processing time. All quantum processing times reported in this study represent simulated quantum processing times obtained through classical simulation using Qiskit, which are orders of magnitude slower than actual Quantum Processing Unit (QPU) execution times. Classical quantum simulation involves exponentially scaling computational overhead that does not reflect the true performance characteristics of real quantum hardware. Real QPU processing could achieve significantly faster execution times, potentially providing computational advantages not captured in our simulation-based validation.

A higher Silhouette Score, as used in Algorithm 1, indicates better-defined clusters. The Fisher Ratio in Algorithm 1 indicates class separability, with higher values suggesting better discrimination between classes. The Davies-Bouldin Index describes the compactness within clusters and the separation between them, and thus, a lower score is desirable. It is defined as follows:

$$DB = \frac{1}{k} \sum_{i=1}^k \max_{j \neq i} \left(\frac{\sigma_i + \sigma_j}{d(c_i, c_j)} \right), \quad (20)$$

where,

- k = number of clusters
- σ_i = average distance of all samples in cluster i to its centroid c_i
- σ_j = average distance of all samples in cluster j to its centroid c_j
- $d(c_i, c_j)$ = distance between centroids c_i and c_j

Initial results show that VQE-derived features currently underperform classical methods like HOG-based and edge-based clustering in metrics such as the Silhouette Score, Davies-Bouldin Index, and Fisher Ratio, though they surpass colour-based clustering. However, these results must be interpreted with significant caution as they are based on classical simulation rather than real quantum hardware execution. Real NISQ devices exhibit substantially higher quantum error rates compared to classical quantum simulators, which could lead to vastly different feature selection quality and convergence behaviour than our simulated results suggest. All quantum processing times reported in this study represent simulated quantum processing times obtained through classical simulation using Qiskit, which are orders of magnitude slower than actual Quantum Processing Unit (QPU) execution times. Classical quantum simulation involves exponentially scaling computational overhead that does not reflect the true performance characteristics of real quantum hardware. Real QPU processing could achieve significantly faster execution times, potentially providing computational advantages not captured in our simulation-based validation. This reveals a critical divergence where classical feature selection methods rely on well-established mathematical frameworks, while quantum-inspired algorithms like VQE require fundamentally different handling. Attempting to directly apply classical statistical paradigms to quantum workflows introduces mismatches in optimisation landscapes and computational paradigms. Instead, VQE should be integrated through hybrid quantum-classical pipelines that leverage classical pre-processing for dimensionality reduction and quantum circuits for specialised feature enhancement [26].

V. CONCLUSION

This quantum workflow demonstrates the feasibility of using variational quantum eigensolvers (VQE) for compact feature extraction in image processing of classical models, achieving dimensionality reduction through optimised quantum circuits while maintaining discriminative power comparable to classical methods, though current performance limitations require honest acknowledgement and systematic future research. The approach successfully integrates adaptive PCA pre-processing with spatially encoded Hamiltonian and gradient-aware parameter pruning, evidenced by a 58 reduction in the Euclidean distance between the pedestrian image features (0.2027 to 0.0841), prioritising high-energy components that capture essential spatial patterns while suppressing noise. However, the current underperformance of the quantum method in clustering metrics (Silhouette Score, Fisher Ratio, Davies-Bouldin Index) stems from NISQ device

constraints that restrict circuit depth and limit processing to 4×4 grayscale patches, preventing capture of complex spatial features essential for real-world objects. To address one of the fundamental limitations, we propose an algorithmic enhancement for future implementation that could significantly improve optimisation performance. The first involves adaptive coefficient initialisation within the VQE optimisation loop, where instead of randomly initialising Hamiltonian weights, classical shadow tomography would estimate operator importance and set initial coefficients proportionally. During each VQE iteration, these coefficients would be dynamically updated based on gradient feedback, creating dual optimisation of both quantum circuit parameters and Hamiltonian weights. Although the current experimental validation underperforms multiple classical approaches used in actual automotive perception systems, future work must prioritize error mitigation techniques like Zero-Noise Extrapolation (ZNE) [27] and systematic adaptive pruning validation to address current accuracy challenges, alongside hardware-optimized implementations and expanded data compatibility.

REFERENCES

- [1] B. Singh and A. Gupta, "Recent trends in intelligent transportation systems: A review," *J. Transp. Literature*, vol. 9, no. 2, pp. 30–34, Apr. 2015.
- [2] W. Wang, N. Cheng, M. Li, T. Yang, C. Zhou, C. Li, and F. Chen, "Value matters: A novel value of information-based resource scheduling method for CAVs," *IEEE Trans. Veh. Technol.*, vol. 73, no. 6, pp. 8720–8735, Jun. 2024.
- [3] Q. Wang, H. Yigitler, R. Jäntti, and X. Huang, "Localizing multiple objects using radio tomographic imaging technology," *IEEE Trans. Veh. Technol.*, vol. 65, no. 5, pp. 3641–3656, May 2016.
- [4] C. Dai, X. Liu, W. Chen, and C.-F. Lai, "A low-latency object detection algorithm for the edge devices of IoV systems," *IEEE Trans. Veh. Technol.*, vol. 69, no. 10, pp. 11169–11178, Oct. 2020.
- [5] Z. Chen, K. Yang, Y. Wu, H. Yang, and X. Tang, "HCLT-YOLO: A hybrid CNN and lightweight transformer architecture for object detection in complex traffic scenes," *IEEE Trans. Veh. Technol.*, vol. 74, no. 3, pp. 3681–3694, Mar. 2025.
- [6] K. Zhang, C. K. M. Lee, Y. P. Tsang, and C. H. Wu, "Variational quantum reinforcement learning for joint resource allocation of blockchain-based vehicular edge computing and quantum internet," *IEEE Trans. Veh. Technol.*, vol. 74, no. 10, pp. 1–16, Oct. 2025.
- [7] A. Galindo and M. A. Martín-Delgado, "Information and computation: Classical and quantum aspects," *Rev. Modern Phys.*, vol. 74, no. 2, pp. 347–423, May 2002.
- [8] A. Peruzzo, J. McClean, P. Shadbolt, M.-H. Yung, X.-Q. Zhou, P. J. Love, A. Aspuru-Guzik, and J. L. O'Brien, "A variational eigenvalue solver on a photonic quantum processor," *Nature Commun.*, vol. 5, no. 1, p. 4213, Jul. 2014.
- [9] J. Zhou, D. Gao, and D. Zhang, "Moving vehicle detection for automatic traffic monitoring," *IEEE Trans. Veh. Technol.*, vol. 56, no. 1, pp. 51–59, Jan. 2007.
- [10] Y. Yao, B. Tian, and F.-Y. Wang, "Coupled multivehicle detection and classification with prior objectness measure," *IEEE Trans. Veh. Technol.*, vol. 66, no. 3, pp. 1975–1984, Mar. 2017.
- [11] Y. Zhang, D. Zhu, P. Wang, G. Zhang, and H. Leung, "Vision-based vehicle detection for VideoSAR surveillance using low-rank plus sparse three-term decomposition," *IEEE Trans. Veh. Technol.*, vol. 69, no. 5, pp. 4711–4726, May 2020.
- [12] N. Pudjihartono, T. Fadason, A. W. Kempa-Liehr, and J. M. O'Sullivan, "A review of feature selection methods for machine learning-based disease risk prediction," *Frontiers Bioinf.*, vol. 2, Jun. 2022, Art. no. 927312. [Online]. Available: <https://www.frontiersin.org/articles/10.3389/fbinf.2022.927312/full>
- [13] S. Mücke, R. Heese, S. Müller, M. Wolter, and N. Piatkowski, "Feature selection on quantum computers," *Quantum Mach. Intell.*, vol. 5, no. 1, p. 11, Feb. 2023.
- [14] Z. Huang, W. Liu, S. Shen, and J. Ma, "A universal cooperative decision-making framework for connected autonomous vehicles with generic road topologies," *IEEE Trans. Veh. Technol.*, vol. 74, no. 4, pp. 5414–5429, Apr. 2025.
- [15] G. Turati, M. F. Dacrema, and P. Cremonesi, "Feature selection for classification with QAOA," in *Proc. IEEE Int. Conf. Quantum Comput. Eng. (QCE)*, Sep. 2022, pp. 782–785.
- [16] H. Wang, "A novel feature selection method based on quantum support vector machine," *Phys. Scripta*, vol. 99, no. 5, Apr. 2024, Art. no. 056006.
- [17] G. Gong, "Variational quantum isometric feature mapping," in *Proc. 4th Int. Symp. Comput. Technol. Inf. Sci. (ISCTIS)*, Jul. 2024, pp. 558–563.
- [18] R. K. Nath, H. Thapliyal, and T. S. Humble, "Quantum annealing for automated feature selection in stress detection," in *Proc. IEEE Comput. Soc. Annu. Symp. VLSI (ISVLSI)*, Jul. 2021, pp. 453–457.
- [19] D. Pan, G.-L. Long, L. Yin, Y.-B. Sheng, D. Ruan, S. X. Ng, J. Lu, and L. Hanzo, "The evolution of quantum secure direct communication: On the road to the qinternet," *IEEE Commun. Surveys Tuts.*, vol. 26, no. 3, pp. 1898–1949, 3rd Quart., 2024.
- [20] P. Botsinis, D. Alanis, Z. Babar, H. V. Nguyen, D. Chandra, S. X. Ng, and L. Hanzo, "Quantum search algorithms for wireless communication," *IEEE Commun. Surveys Tuts.*, vol. 21, no. 2, pp. 1209–1242, 2nd Quart., 2019.
- [21] A. Kulshrestha, X. Liu, H. Ushijima-Mwesigwa, B. Bach, and I. Safro, "Qadaprune: Adaptive parameter pruning for training variational quantum circuits," in *Proc. IEEE Int. Conf. Quantum Comput. Eng.*, Jul. 2024, pp. 120–125.
- [22] N. Dalal and B. Triggs, "Histograms of oriented gradients for human detection," in *Proc. IEEE Comput. Soc. Conf. Comput. Vis. Pattern Recognit.*, vol. 1, Jun. 2005, pp. 886–893.
- [23] K. R. Shahapure and C. Nicholas, "Cluster quality analysis using silhouette score," in *Proc. IEEE 7th Int. Conf. Data Sci. Adv. Analytics (DSAA)*, Oct. 2020, pp. 747–748.
- [24] D. L. Davies and D. W. Bouldin, "A cluster separation measure," *IEEE Trans. Pattern Anal. Mach. Intell.*, vols. PAMI-1, no. 2, pp. 224–227, Apr. 1979.
- [25] M. R. B. Clarke, "Pattern classification and scene analysis," *J. Roy. Stat. Soc., Ser. A (General)*, vol. 137, no. 3, pp. 442–443, 1974.
- [26] D. Slabbert and F. Petruccione, "Classical-quantum approach to image classification: Autoencoders and quantum SVMs," *AVS Quantum Sci.*, vol. 7, no. 2, Jun. 2025, Art. no. 023804.
- [27] T. Pandey, J. Saroni, A. Kazi, and K. Sharma, "Efficient variational quantum eigensolver methodologies on quantum processors," 2024, *arXiv:2407.16107*.



VIKAS HASSIJA received the M.E. degree from the Birla Institute of Technology and Science-Pilani, Pilani, India, in 2014. He was a Post-doctoral Research Fellow with the National University of Singapore (NUS), Singapore. He is currently an Associate Professor with the School of Computer Engineering, Kalinga Institute of Industrial Technology, Bhubaneswar, India. His current research interests include blockchain, non-fungible tokens, the IoT, privacy and security, and distributed networks.



AVISHIKTA BHATTACHARJEE is currently pursuing the B.Tech. degree in computer science and engineering (CSE) from the Kalinga Institute of Industrial Technology (KIIT), Bhubaneswar.



ARADHYA CHAKRABARTI is currently pursuing the B.Tech. degree in computer science and engineering (CSE) from the Kalinga Institute of Industrial Technology (KIIT), Bhubaneswar.



M. ADHITYA is currently pursuing the B.Tech. degree in computer science and engineering from the Kalinga Institute of Industrial Technology, Bhubaneswar. His primary research interests include large language models, deep learning, and natural language processing. In addition to his academic and research work, he enjoys problem-solving and exploring innovative applications of artificial intelligence.



QAISER RAZI (Graduate Student Member, IEEE) received the M.E. degree from the Birla Institute of Technology, Mesra, Ranchi, India, in 2019. He is currently pursuing the Ph.D. degree with the Department of Electrical and Electronics Engineering, BITS-Pilani, Pilani, India. He is a Research Scholar with the Department of Electrical and Electronics Engineering, BITS-Pilani. His research interests include artificial intelligence, privacy and security, the IoT, and non-fungible tokens.



G. S. S. CHALAPATHI (Senior Member, IEEE) received the B.E. degree (Hons.) in electrical and electronics engineering, the M.E. degree in embedded systems, and the Ph.D. degree from the Birla Institute of Technology and Science (BITS), Pilani, in 2009, 2011, and 2019, respectively. He carried out his postdoctoral research with The University of Melbourne, Australia, under the supervision of Prof. Rajkumar Buyya, and a Distinguished Professor with The University of Melbourne. During his doctoral studies, he was a Visiting Researcher with the National University of Singapore and Johannes Kepler University, Austria. He has published in reputed journals, such as *IEEE WIRELESS COMMUNICATIONS LETTERS*, *IEEE SENSORS JOURNAL*, and *Future Generation Computing Systems*. His research interests include UAVs, precision agriculture, and embedded systems. He is a member of ACM. He is a reviewer of *IEEE INTERNET OF THINGS JOURNAL* and *IEEE ACCESS*.

• • •